A Novel Electrolyte Additive Enables High Voltage Operation of Nickel-rich Oxide/Graphite Cell

Zhangmin Hu[#,a], Kang Wang[#,a], Yanxia Che[a], Mingzhu Liu[a], Wenguang zhang[a], Lidan Xing[a,b], Hai Wang[c], Suli Li[c], Xiang Liu[d,*], Weishan Li[a,b,*]

[a] *School of Chemistry, South China Normal University, Guangzhou 510006, China*

[b] *National and Local Joint Engineering Research Center of MPTES in High Energy and Safety LIBs, Engineering Research Center of MTEES (Ministry of Education), and Key Lab. of ETESPG(GHEI), South China Normal University, Guangzhou 510006, China*

[c] *Zhuhai CosMX Battery Co., Ltd, Zhuhai 519180, China*

[d] *College of Energy Science and Engineering, Nanjing Tech University, 30 Puzhu South Road, Nanjing 211816, China*

Corresponding Authors: iamxliu@njtech.edu.cn; liwsh@scnu.edu.cn

Author Contributions

[#] Zhangmin Hu and Kang Wang contributed equally to this work

Figure captions

Figure S1. Electrochemical cell for differential electrochemical mass spectroscopy (DEMS).

Figure S2. Changes in the thickness of NCM523/graphite pouch cells cycled at a rate of 1C under 25 °C in baseline electrolyte between 2.75-4.2 V (a), 2.75-4.35 V (b), 2.75-4.5 V (c), and in NOB-containing electrolyte between 2.75-4.2 V (d), 2.75-4.35 V (e), 2.75-4.5 V (f).

Figure S3. Cycle stability of NCM523/graphite pouch cells with baseline and NOB-containing electrolytes under 1C at 25 °C with an additional constant voltage step to 0.1 C at the end-off charge voltages, 2.75-4.2 V.

Figure S4. Cycle stability of $LiCoO_2$/Li cells with baseline and NOB-containing electrolytes under 1C at 25 °C between 3 and 4.5 V (a). chronoamperometric responses at 4.5 V (b, c).

Figure S5. Electrochemical impedance spectra of NCM523/graphite pouch cells in baseline (a) and NOB-containing (b) electrolytes during cycling test of Figure 1c at the 3^{rd} (a) and 100^{th} (b) cycle.

Figure S6. Charge/discharge curves of NCM523/graphite pouch cells at 25 °C under different charge currents in a constant current/voltage charge mode but at the same discharge current in baseline (a) and NOB-containing (b) electrolytes. Ratios of the charge capacity under constant current to the total charge capacity (c).

Figure S7. Charge/discharge curves of NCM523/graphite pouch cells at 25 °C under the same charge current in a constant current/voltage charge mode but at different discharge currents in baseline (a) and NOB-containing (b) electrolytes. Dependence of discharge capacity on discharge currents (c).

Figure S8. Color changes of the baseline electrolytes with immersing the fully charged cathodes taken from the cells after formation process, the immersion was performed at 45 °C for 72 h.

Figure S9. XRD patterns of fresh and the NCM electrodes cycled in baseline and NOB-containing electrolytes for 100 cycles under 4.5 V.

Figure S10. XPS profiles of C 1s, O 1s, F 1s, P 2p, N 1s, and Si 2p for NCM523 after 100 cycles at 1C in baseline and NOB-containing electrolytes between 2.75-4.5 V.

Figure S11. Gas chromatograms of the electrolyte taken from the cycled cell in the NOB-containing electrolyte after formation process, with a comparison of the fresh NOB-containing electrolyte.

Figure S12. Optimized structures and adiabatic ionization energy (AIE, kJ mol^{-1}) of NOB.

Figure S13. Optimized structures and adiabatic ionization energy (AIE, kJ mol^{-1}) of X, X=EC, EMC, DEC, and $Si(CH_3)_3F$.

Table S1. A comparison of electrolyte additives for improving cycle stability of high-nickel oxide/graphite cells under high voltages.

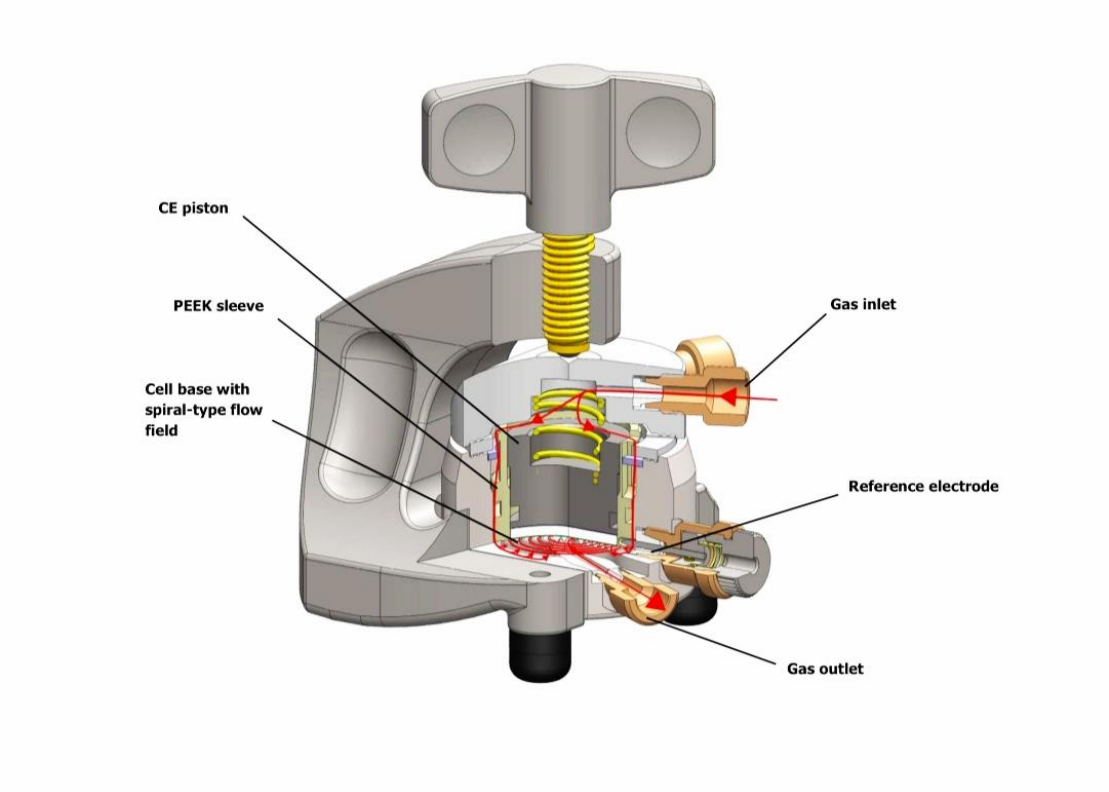

Figure S1. The inner structure of the electrochemical cell used for differential electrochemical mass spectroscopy (DEMS).

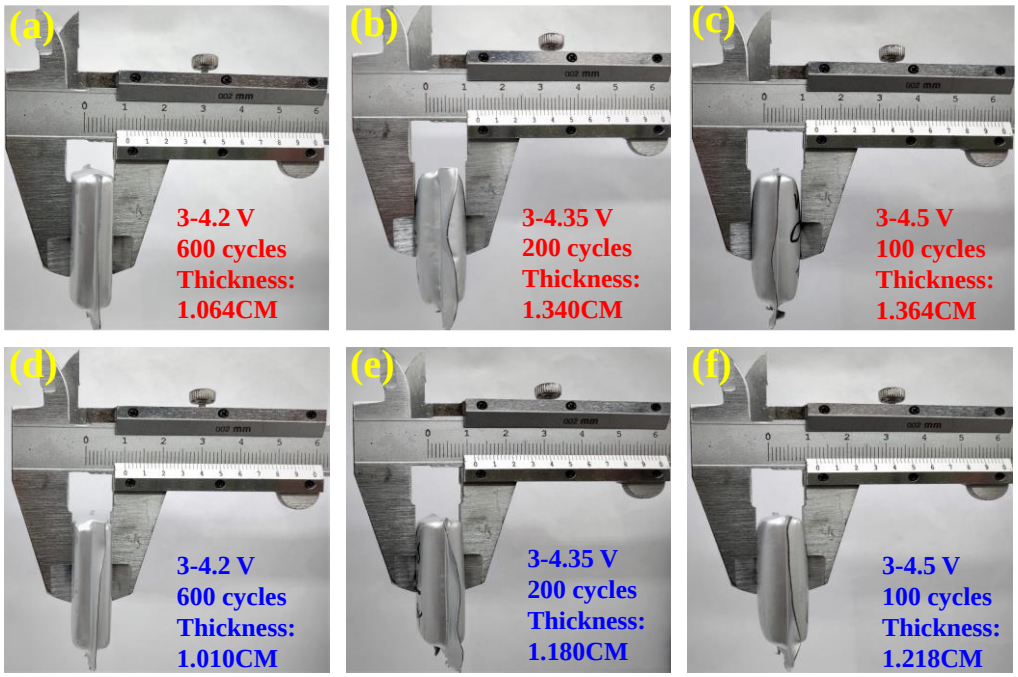

Figure S2. Changes in the thickness of NCM523/graphite pouch cells cycled at a rate of 1C under 25 °C in baseline electrolyte between 2.75-4.2 V (a), 2.75-4.35 V (b), 2.75-4.5 V (c)，and in NOB-containing electrolyte between 2.75-4.2 V (d), 2.75-4.35 V (e), 2.75-4.5 V (f).

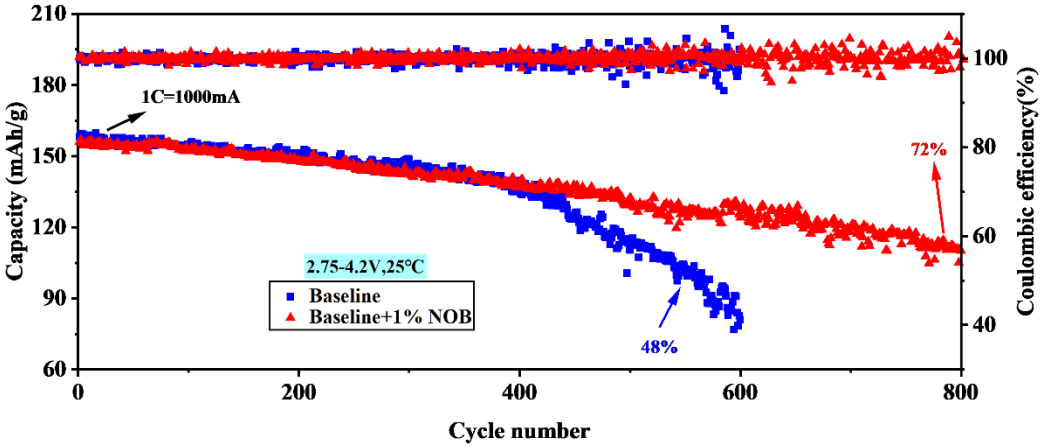

Figure S3. Cycle stability of NCM523/graphite pouch cells with baseline and NOB-containing electrolytes under 1C at 25 °C with an additional constant voltage step to 0.1 C at the end-off charge voltages, 2.75-4.2 V.

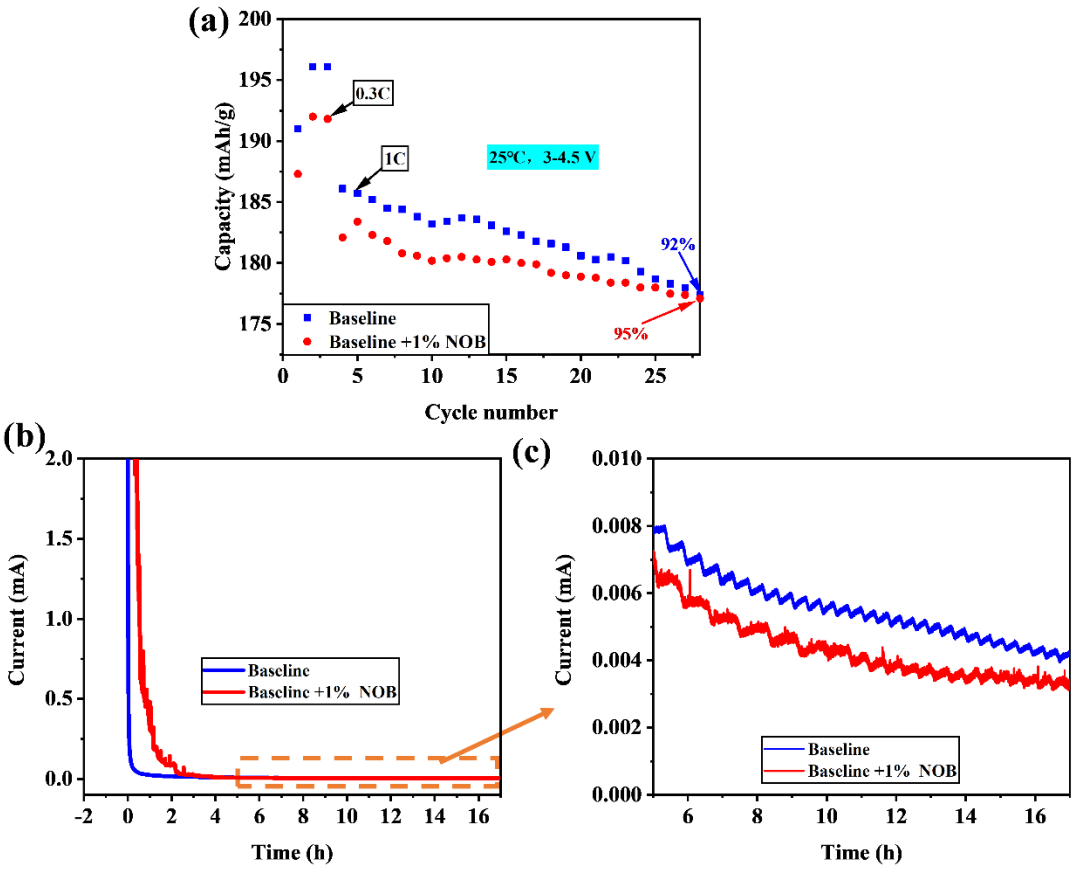

Figure S4. Cycle stability of $LiCoO_2$/Li cells with baseline and NOB-containing electrolytes under 1C at 25 °C between 3 and 4.5 V (a). chronoamperometric responses at 4.5 V (b, c).

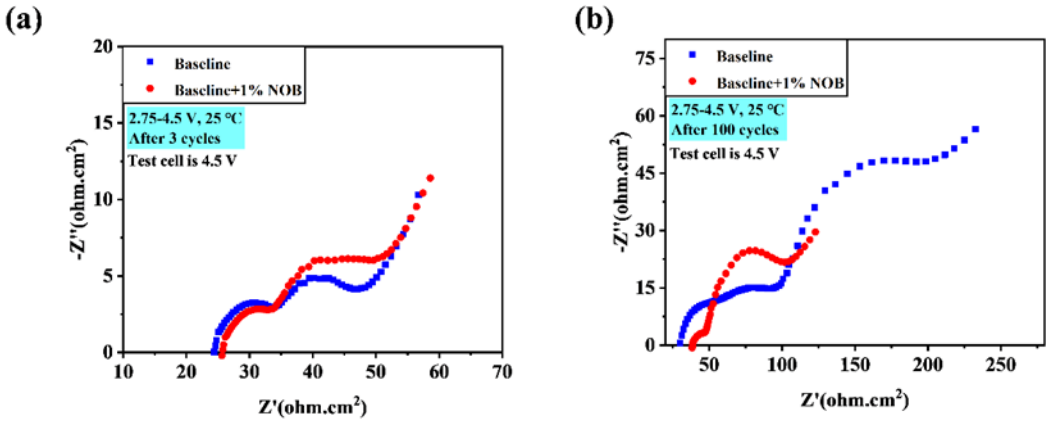

Figure S5. Electrochemical impedance spectra of NCM523/graphite pouch cells in baseline (a) and NOB-containing (b) electrolytes during cycling test of Figure 1c at the 3rd (a) and 100th (b) cycle.

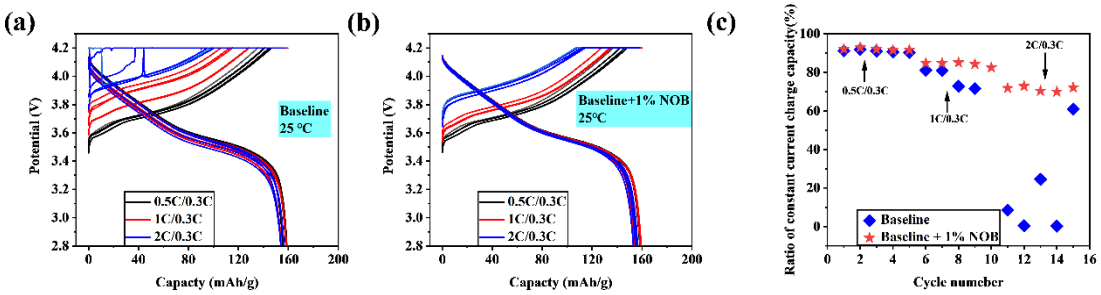

Figure S6. Charge/discharge curves of NCM523/graphite pouch cells at 25 °C under different charge currents in a constant current/voltage charge mode but at the same discharge current in baseline (a) and NOB-containing (b) electrolytes. Ratios of the charge capacity under constant current to the total charge capacity (c)

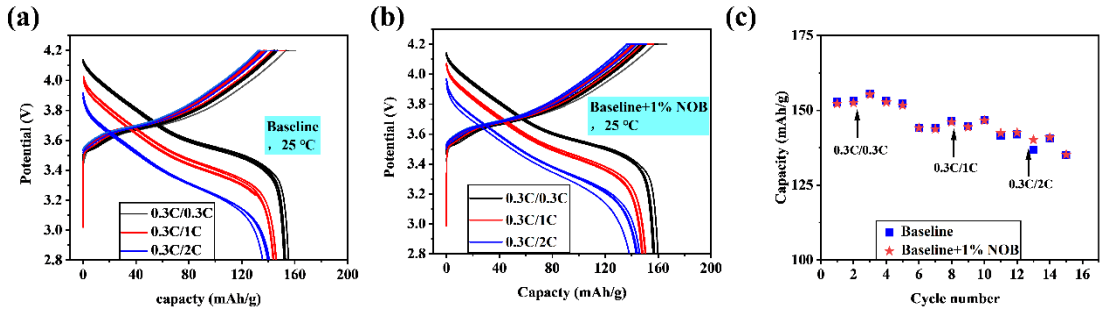

Figure S7. Charge/discharge curves of NCM523/graphite pouch cells at 25 °C under the same charge current in a constant current/voltage charge mode but at different discharge currents in baseline (a) and NOB-containing (b) electrolytes. Dependence of discharge capacity on discharge currents (c).

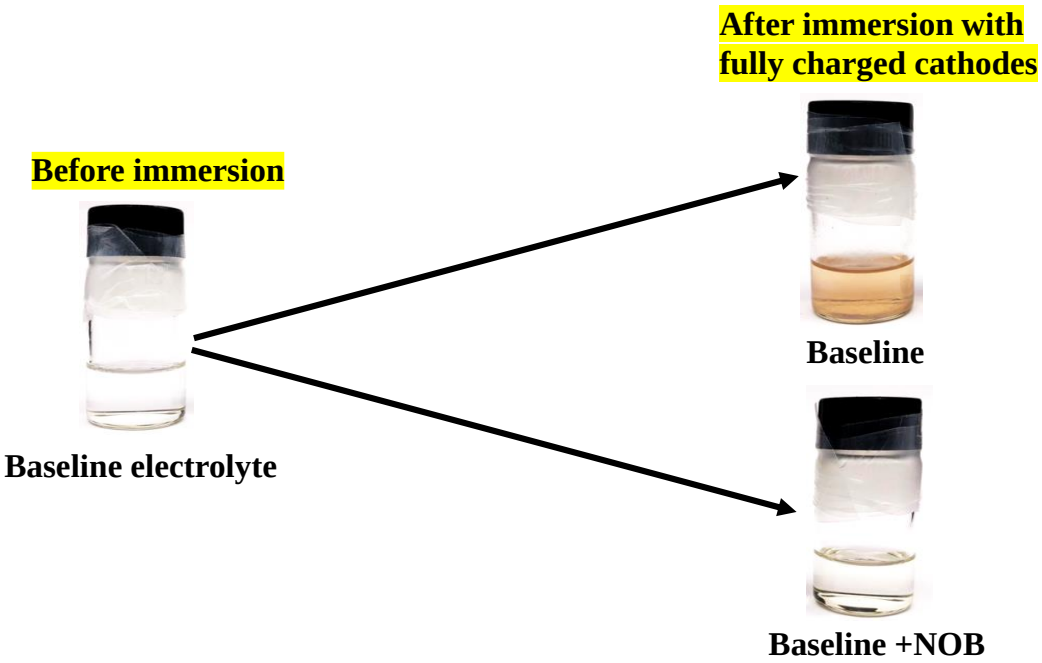

Figure S8. Color changes of the baseline electrolytes with immersed the fully charged cathodes taken from the cells after formation process, the immersion was performed at 45 °C for 72 h.

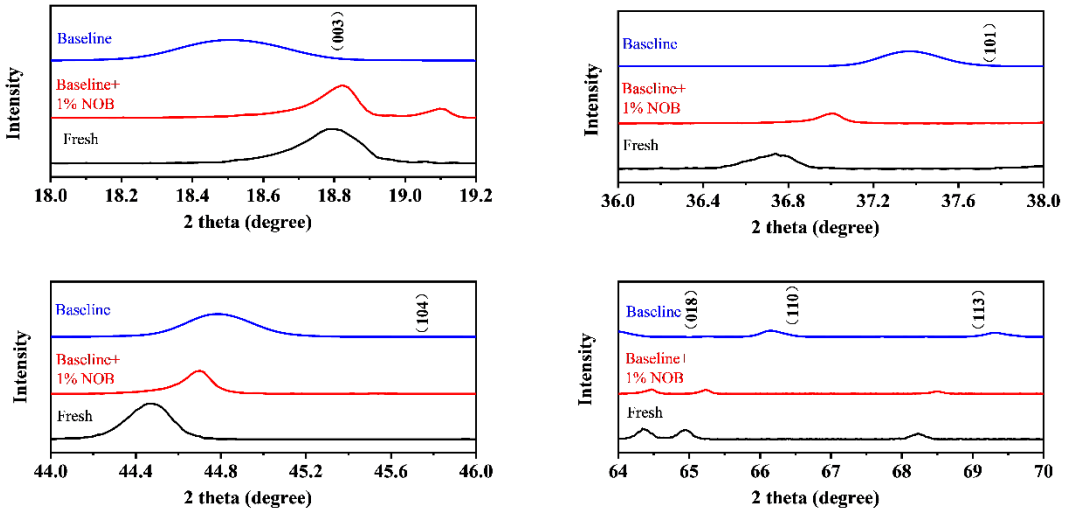

Figure S9. XRD patterns of fresh and the NCM electrodes cycled in baseline and NOB-containing electrolytes for 100 cycles under 4.5 V.

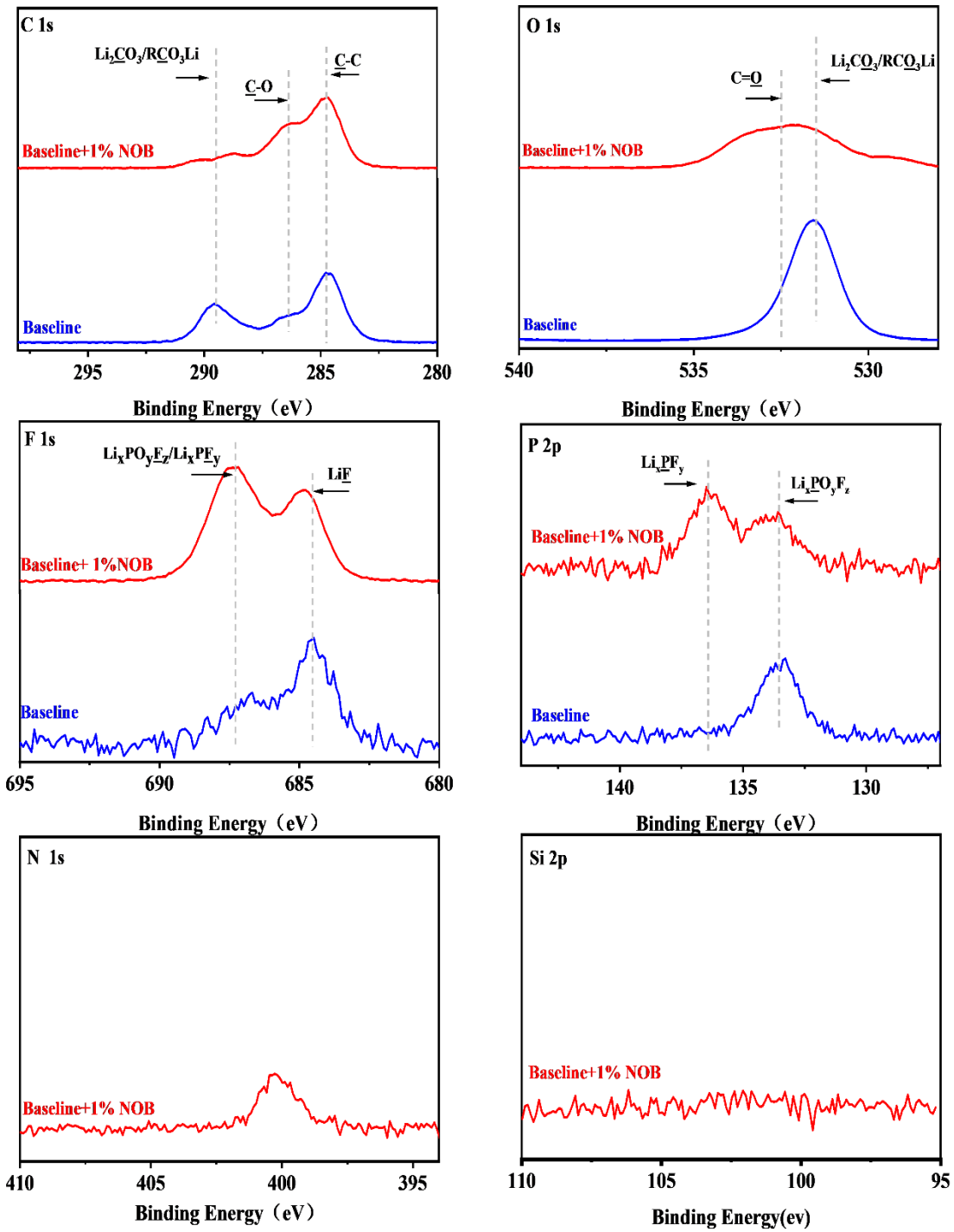

Figure S10. XPS profiles of C 1s, O 1s, F 1s, P 2p, N 1s, and Si 2p for graphite after 100 cycles at 1C in baseline and NOB-containing electrolytes between 2.75-4.5 V.

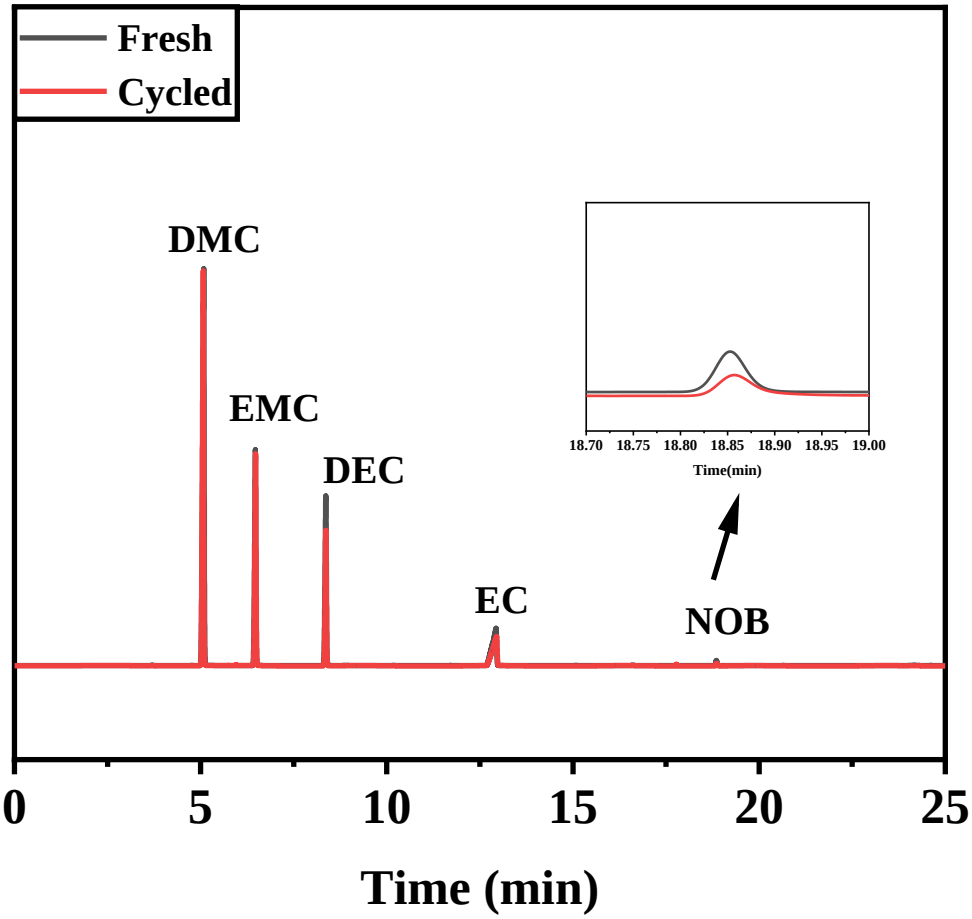

Figure S11. Gas chromatograms of the electrolyte taken from the cycled cell in the NOB-containing electrolyte after formation process, with a comparison of the fresh NOB-containing electrolyte.

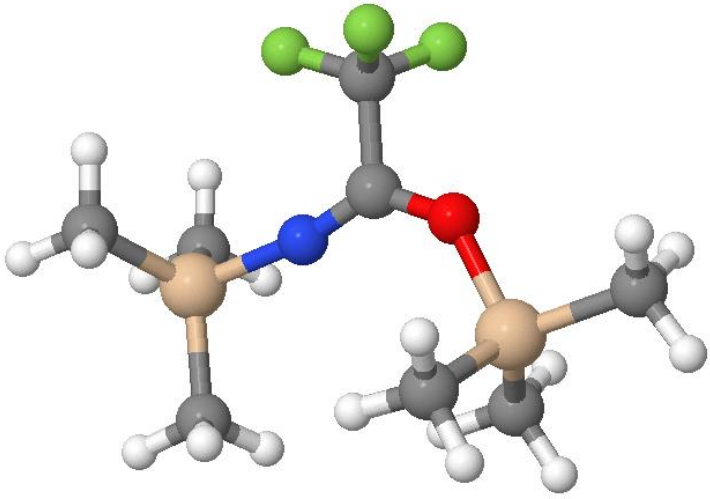

$AIE_{(NOB)}$=640

Figure S12. Optimized structures and adiabatic ionization energy (AIE, kJ mol^{-1}) of NOB.

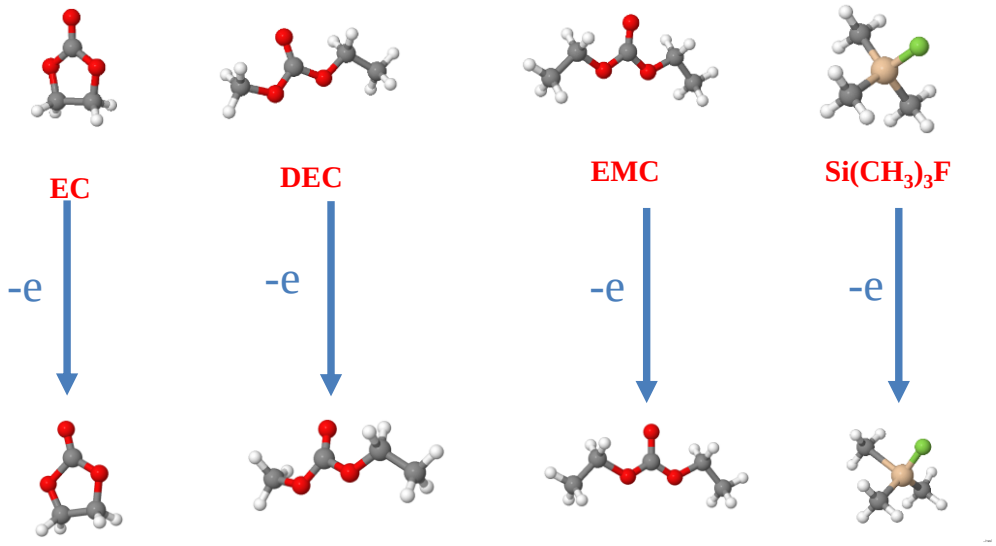

Figure S13. Optimized structures and adiabatic ionization energy (AIE, kJ mol^{-1}) of X, X=EC, EMC, DEC, and $Si(CH_3)_3F$.

Table S1 A comparison of electrolyte additives for improving high voltage cycle stability of high-nickel oxide/graphite cells.

Electrolyte Additive	Cell	Voltage Range(V)	Current rate (C)	Cycle Number	Capacity Retention Improvement
N,O-bis(trimehylsilyl)- trifluoroacetamide (NOB) (This work)	Graphite/NCM523	2.75-4.2 V	1	600	30%
N,O-bis(trimehylsilyl)- trifluoroacetamide (NOB) (This work)	Graphite/NCM523	2.75-4.5 V	1	100	35%
N,N-diethylamino trimethylsilane(DEATMS) 【39】	Graphite/NCM523	3-4.5 V	1	100	14%
Lithium difluorophosphate ($LiPO_2F_2$) 【40】	Graphite/NCM523	3-4.4V	1	150	28%
tris(2,2,2-trifluoroethyl) phosphite (TTFP) 【41】	Graphite/NCM523	3-4.6 V	1	50	5%
2,3,4,5,6-Pentafluorophenyl Methanesulfonate (PFPMS) 【42】	Graphite/NCM523	3-4.2 V	1	400	17%
vinylene carbonate (VC) 【42】	Graphite/NCM523	3-4.2 V	1	400	2%
1,4-Dicyanobutane (ADN) 【43】	Graphite/NCM523	3-4.4 V	1	120	17%